Mono- and Multilayers of Mesogen-Substituted Carbosilane Dendrimers on Mica

Martine Collaud Coen, Klaus Lorenz, Jörg Kressler, Holger Frey,* and Rolf Mülhaupt

Institut für Makromolekulare Chemie und Materialforschungszentrum FMF, Albert-Ludwigs-Universität Freiburg, Stefan-Meier-Str. 21/31, D-79104 Freiburg, FRG

Received October 17, 1995; Revised Manuscript Received September 26, 1996[⊗]

ABSTRACT: Self-assembled ultrathin (5−15 nm) films of carbosilane dendrimers with mesogenic units on the periphery, obtained after deposition on mica surfaces, have been studied with atomic force microscopy. Dendritic polymers with 12, 36, and 108 mesogenic cholesteryl end groups, first, second, and third generation, respectively, were employed. Solvent casting was used to generate the films. At high concentrations of the dendrimers in solution, flat, homogeneous films of 2−4 dendrimer layers were found. For low dendrimer concentrations, a single dendrimer monolayer exhibiting an irregular cellular pattern of holes was observed. The thickness of the monolayer correlated well with the diameter of the dendrimers and with wide-angle X-ray scattering results obtained on crystalline powders. Annealing of the films of G1 and G2 in the liquid crystalline phase caused reorientation of the molecules at the surface. The third-generation dendrimer with 108 end groups (G3), the periphery of which is densely packed with mesogens, behaved differently and did not show dewetting or reorientation upon annealing, which is attributed to lower molecular mobility.

Introduction

The adsorption of linear macromolecules on surfaces has motivated several experimental and theoretical studies.[1,2] Dependent on their molecular architecture, most polymers show tendencies toward self-organization in a variety of lamellar or even uniaxial supramolecular structures.[3] This is utilized in the fabrication of ultrathin, ordered molecular films with specific surface functionality.[4]

Dendrimers, also termed "starburst polymers" or "arborols" possess a highly branched molecular topology[5,6] and physical properties that are determined by their globular, spherical shape. Peculiar features of the dendritic geometry are the large number of end groups as well as the shape persistence in higher generations, approaching spherical geometry.

Generally, it is surprising that the condensed phase behavior of dendrimers has scarcely been investigated. Although the deposition of dendrimers on surfaces appears intriguing because of their unusual shape persistence and multiple intermolecular interactions as well as the lack of chain entanglements, little information is available at present on ordering of dendrimers on surfaces. The formation of monolayers and ultrathin molecularly flat films are interesting issues in this context. Watanabe and Regen[7] as well as Kowalewski et al.[8] in a preliminary account demonstrated the formation of layers of dendrimers on surfaces. Sheiko et al. reported on the formation of ordered morphologies for liquid carbosiloxane dendrimers on various surfaces,[9] studied by atomic force microscopy (AFM).

We have recently reported on dendritic liquid crystalline polymers (DLCP), based on a flexible, dendritic carbosilane scaffold, to which rigid, anisotropic units (mesogens) are attached.[10] Formally, the formisotropic geometry of dendrimers contradicts the requirements of the liquid crystalline state; however, we observed that cooperative deformation of the macromolecules due to favorable mesogen−mesogen interaction leads to crystalline order as well as thermotropic liquid crystalline phases.

[⊗] Abstract published in *Advance ACS Abstracts,* November 1, 1996.

The present paper summarizes the results of a systematic AFM study on ultrathin films of mesogen-substituted carbosilane dendrimers. The films were generated by simple solvent casting on mica and thus represent nonequilibrium structures. Three generations, namely G1, G2, and G3 with 12, 36, and 108 end groups, respectively, have been used for the current study. We have also studied the thermal behavior of the self-assembled films upon annealing in the liquid crystalline and isotropic state.

Experimental Section

A detailed description of the synthesis of the dendrimers with liquid crystalline groups as well as an account of polydispersities [matrix-assisted laser desorption and ionization−time of flight (MALDI−TOF) detection] and formation of liquid crystalline phases has been given elsewhere.[10]

Solutions of the dendrimers in the concentration range of $0.2-1 \times 10^{-4}$ wt % were prepared in toluene, petroleum ether, chloroform, and *n*-pentane. For the AFM measurements, simple deposition of the solutions on mica and subsequent drying under ambient conditions was employed. Mica substrates possess a flat and crystalline surface and can easily be distinguished from the dendrimer films.

Annealed samples were annealed at 105 °C, i.e. in the liquid crystalline state for the G1 and G2 dendrimers and in the isotropic phase for G3. Different annealing times correspond to succeeding periods of annealing. When the films appeared to be unchanged after annealing at 105 °C, they were heated further to 150 °C (isotropic phase for all generations).

Ambient-condition AFM measurements were conducted with an atomic probe microscope Nanoscope III (Digital Instruments Inc.) in the contact (CMAFM) and tapping modes (TMAFM).[11] Experiments in the contact mode showed that due to the strong forces applied, the sample was destroyed after the first scan. For the contact mode measurements, we employed moderate forces in the 20−40 nN range. In some cases we deliberately applied stronger forces (>100 nN) to remove adsorbed material from the substrate. Detailed information about AFM on soft surfaces in the tapping and contact modes may be found elsewhere.[12] However, unless mentioned otherwise, the measurements in this study were performed with TMAFM. Tips were supplied by Digital Instruments. For the tapping mode studies, short and rigid cantilevers with resonance frequency in the 300−350 kHz range were typically used.

S0024-9297(95)01545-2 CCC: $12.00

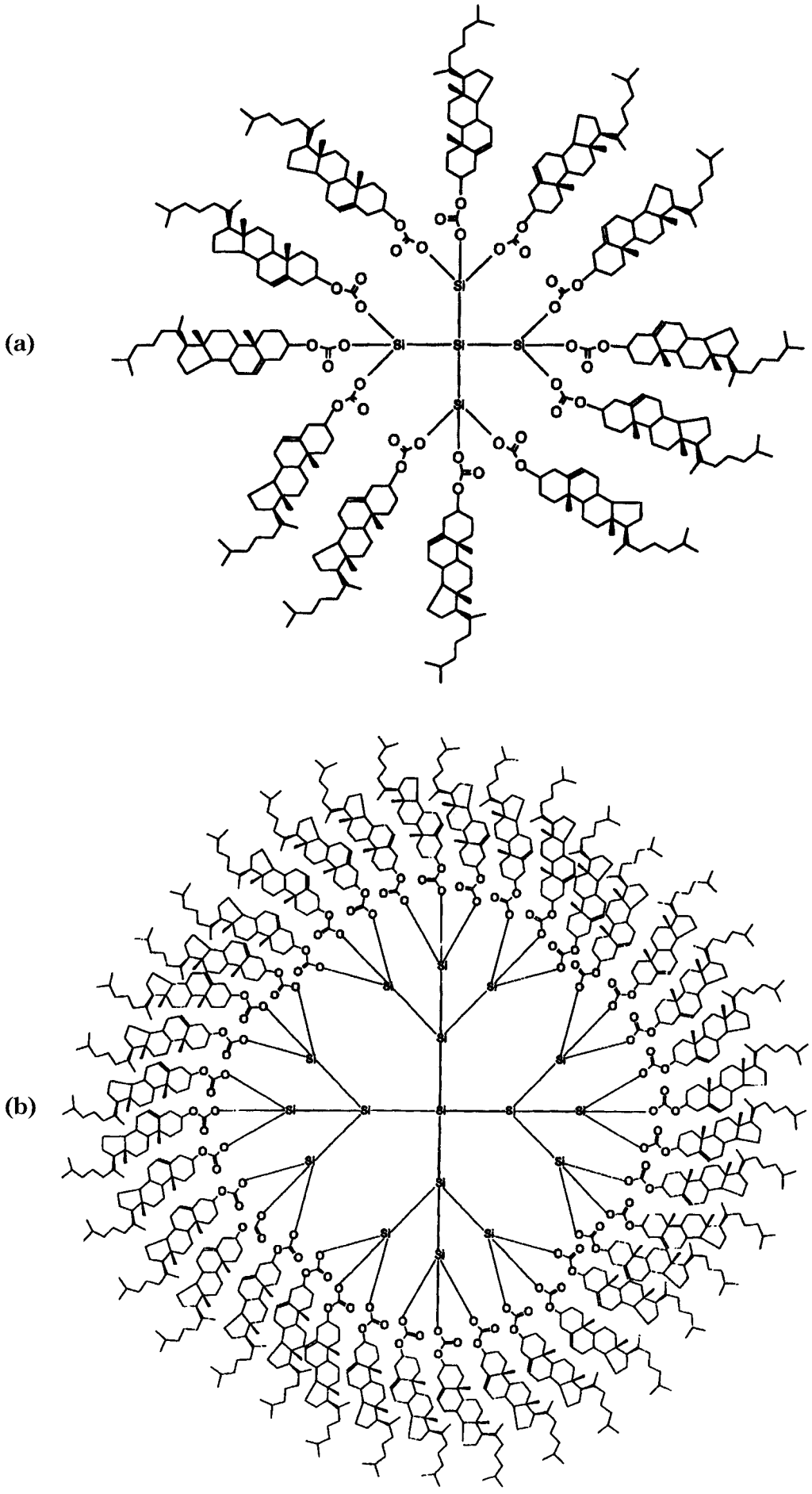

Figure 1. Schematic representation of the dendrimers of G1 (a) and G2 (b) (——— represents a C_3H_6 unit).

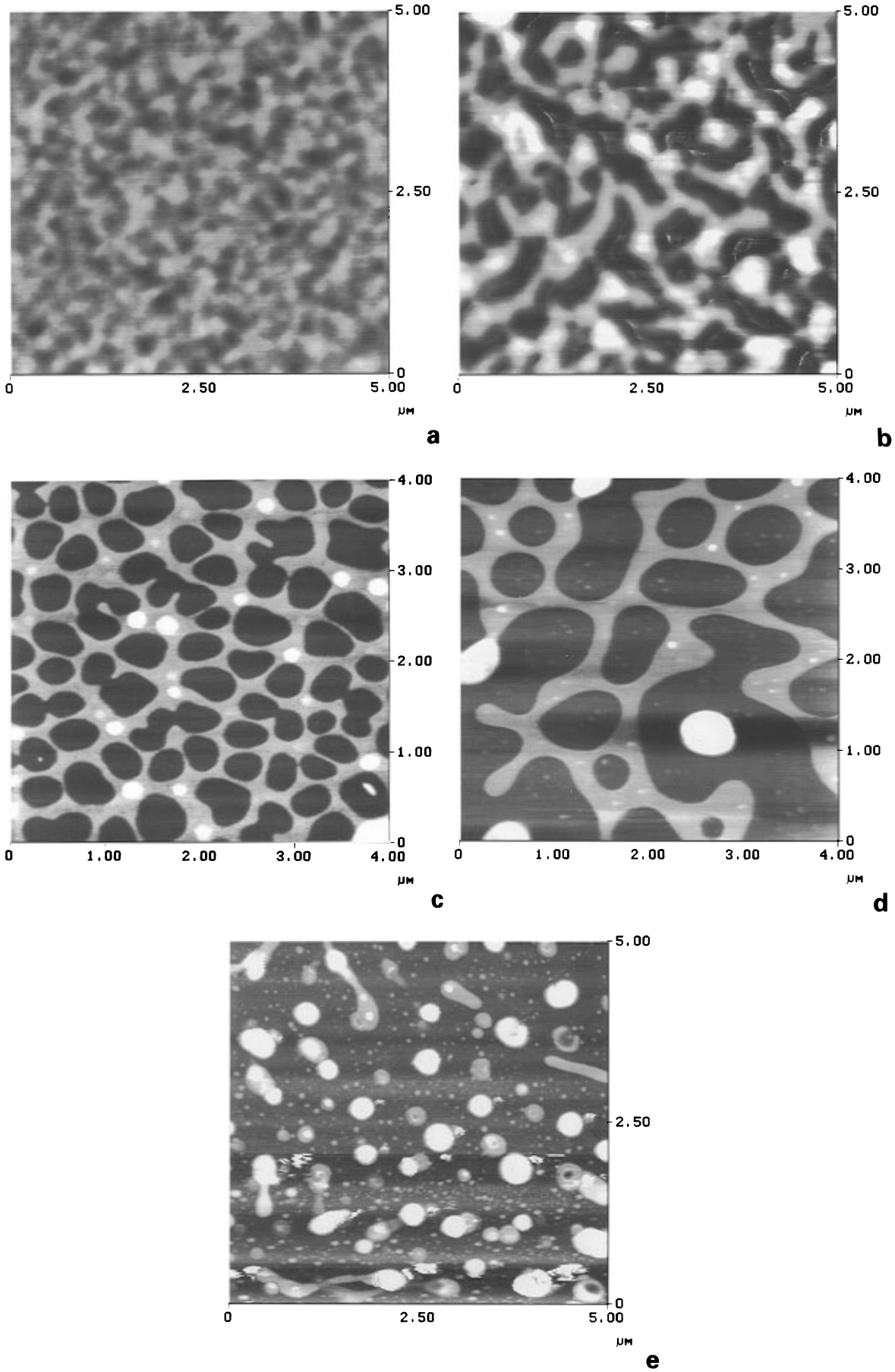

Figure 2. TMAFM images of G2 dendrimers on mica surfaces. The films were deposited by solvent casting from a petroleum ether solution of various dendrimer concentrations: (a) 0.2 wt %, (b) 0.025 wt %, (c) 0.0185 wt %, (d) 0.0125 wt %, and (e) 0.003 wt %.

Table 1. Roughness of 5 μm × 5 μm Area as a Function of the Concentration of a Benzin Solution of G2 Dendrimers

dendrimer concentration (wt %)	rms value (nm)	dendrimer concentration (wt %)	rms value (nm)
0.2	0.7	0.018	2.4
0.1	0.7	0.012	3.0
0.05	3.8	0.006	1.4
0.025	9.1	0.003	3.2

Due to several reasons (thermal noise, calibration accuracy, etc.) the accuracy of the parameters derived from the AFM images is ±10%. This accuracy is estimated from AFM studies of different layered materials (mica, graphite, chalcogenides, and halides of transition metals) with known surface lattices.

Results and Discussion

A divergent synthetic approach based on alternating hydrosilylation/Grignard reaction was employed to prepare the carbosilane dendrimers.[13,14] Subsequently, hydroboration reaction led to quantitative surface hydroxylation of the molecules.[15] Condensation with cholesteryl chloroformate was used to attach the mesogenic units to the surface of the dendrimers. The dendritic liquid crystalline polymers were characterized with respect to structural perfection using conventional NMR techniques as well as MALDI-TOF mass spectroscopy. Divergent synthesis of dendrimers commonly results in an increase of structural defects in higher generations.[15] Whereas G1 consisted of one single species with 12 end groups, G2 consisted of five discrete molecules, bearing 32−36 end groups. G3 possessed a polydispersity of 1.03 and consisted of molecules bearing between 92 and 108 cholesteryl mesogens; the main fraction was substituted with 100−108 mesogens.[10] The perfect structures of the dendrimers of the first and second generation (G1 and G2) used for this study are shown in Figure 1 (G3 is not displayed).

The mesogenic units attached to the periphery of the dendrimers generally induced ordering, i.e. formation of crystalline and liquid crystalline phases. Both G1 and G2 are crystalline powders at ambient temperature and form smectic mesophases, with transition temperatures between 80 and 90 °C. Isotropization is observed at 130 °C for both G1 and G2. G3 did not show the formation of mesophases, which we interpret as a consequence of increasingly spherical geometry of the higher generations.[10] In contrast, the unmodified carbosilane dendrimers are liquids even at low temperatures and possess T_g's below −100 °C. The cholesteryl-substituted dendrimers exhibit excellent solubility in common apolar organic solvents, such as toluene, petroleum ether, and *n*-pentane, which is explained by the solubilizing alkyl chains attached to the cholesteryl mesogens.

Solutions of different concentrations of dendrimers (G1−G3) in the range $0.2-1 \times 10^{-4}$ wt % were used to cast films of different thickness on mica substrates. Figure 2 shows AFM images of the dried films obtained from the G2 dendrimer from petroleum ether solutions with gradually lowered concentration. At the highest concentration of 0.2 wt % (Figure 2a), a film composed of several dendrimer layers is homogeneously formed on the mica surface. This film is very flat and its roughness [root mean square (rms) value of the height of the surface] is 0.7 nm for a 5 μm × 5 μm area (see Table 1). The visible surface inhomogeneities have a height of 0.5−1 nm. Thus, the films are extremely flat, even when compared to PAMAM (polyamidoamine) dendrimer films obtained by sequential deposition.[7]

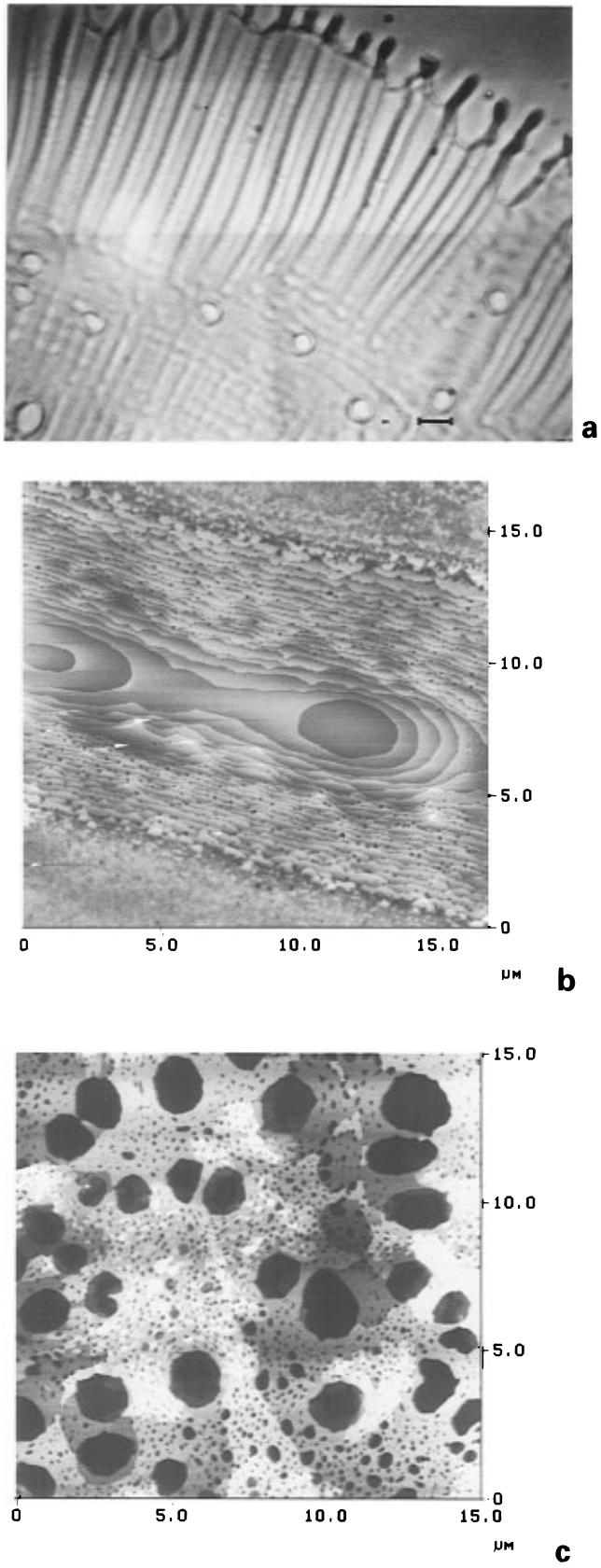

Figure 3. Marangoni instability patterns: (a) optical microscopy (scale bar represents 50 μm) and TMAFM images of (b) 0.1 wt. % of G1 in $CHCl_3$ and of (c) 0.006 wt % of G3 in toluene.

When the films are prepared from a 0.025 wt % solution (Figure 2b), the surface presents a structure similar to a spinodal decomposition pattern, and the polymer domains show organization similar to a cocontinuous phase morphology[16]. In Figure 2b−e the dendrimer concentration was gradually lowered to study the con-

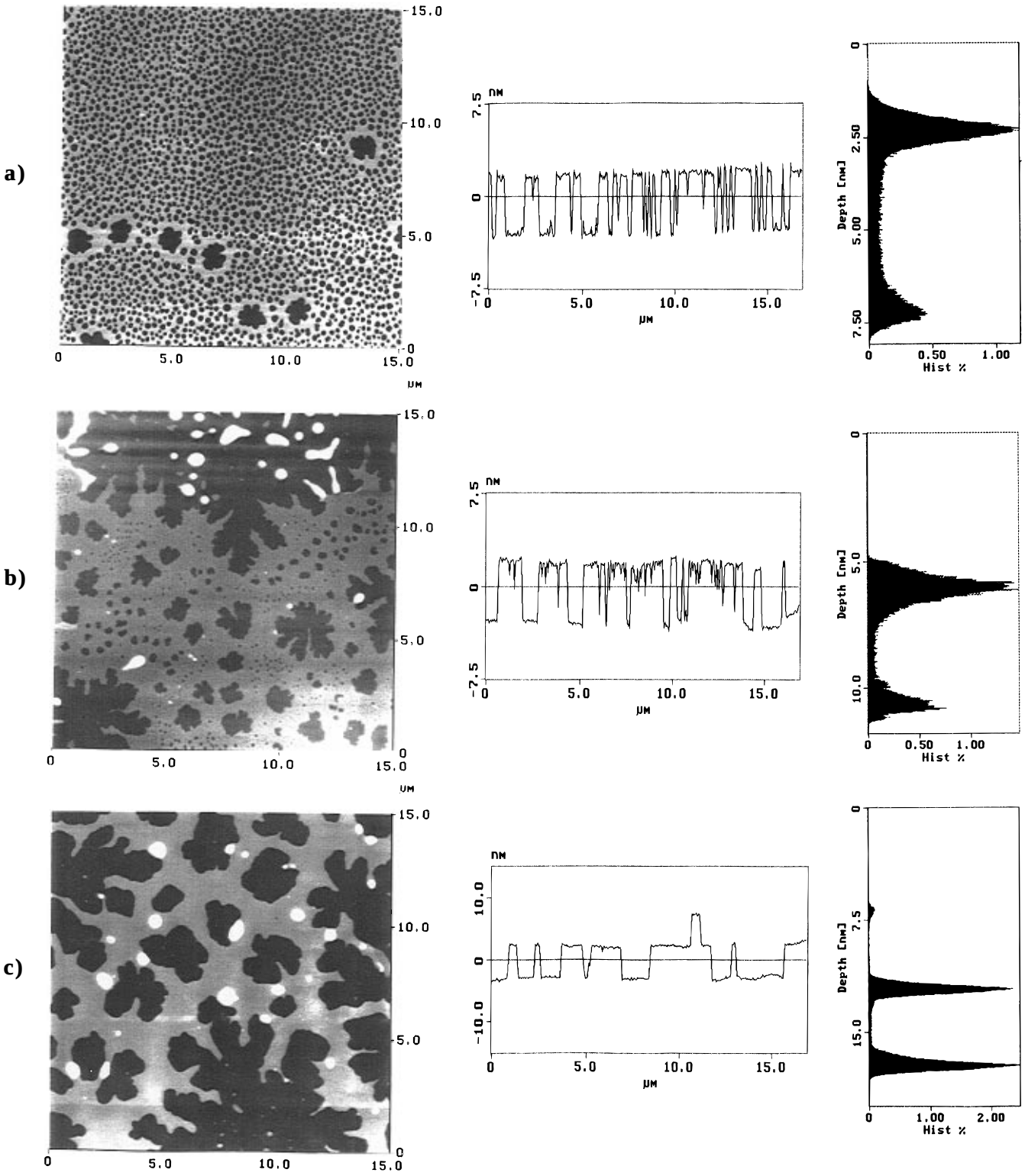

Figure 4. Tapping mode AFM images with corresponding 2D profiles and distribution of the height of the measured points. (a) 0.0015 wt % G1 dendrimers in toluene, (b) 0.012 wt % G2 dendrimers in chloroform, (c) 0.012 wt % G3 dendrimers in toluene.

centration dependence of the film structure. The solvent has evaporated to reveal the mica substrate. The resultant surface due to a kinetic process (dewetting)[16] is therefore rough (rms = 9 nm) in comparison to the extremely flat surface shown in Figure 2a. If the dendrimer concentration is further decreased, a thin layer with holes is obtained (Figure 2c corresponds to a concentration of 0.018 wt %). Although the holes are uniformly distributed on the whole surface, their size is not uniform. The holes shown in Figure 2c have a diameter of approximately 50−60 nm, but holes of 20−30 nm are also found in other areas of the surface. The dendritic film forms a continuous phase, and the holes are the dispersed "phase". The cellular pattern observed by AFM shows similarity with "bubble" patterns observed for LB films at the air/water interface[19] studied by fluorescence microscopy. This 2D character of the systems will be discussed below. For a 0.012 wt % concentration (Figure 2d), the dendrimer film remains continuous, but the holes coalesce to form larger, irregular domains. Finally, at very low concentrations (Figure 2e corresponds to a concentration of 0.003 wt %), a phase inversion occurs: the dendritic film forms island structures and the mica surface forms a continu-

ous medium. The dendrimer droplets are composed of one or two layers of dendrimers, which will be discussed in detail below.

The concentration dependence of the structures formed is summarized in Table 1, which gives the roughness at different concentrations. Clearly, the films are flat at high concentrations, where a multilayer film is created. The roughness increases at intermediate concentrations under the influence of kinetic processes, such as dewetting. This leads to structures similar to spinodal decomposition, which is a cooperative process involving several layers of dendrimers. At lower concentrations, the roughness decreases again with decreasing concentration and characteristic Voronoi structures are formed[17] The presence of these Voronoi tessellations indicates that film rupture occurs almost simultaneously across the entire surface.

This dependence of the film structure on the concentration was typical for all dendrimer generations, when cast from solvents with low vapor pressure. At high concentrations, the regular formation of multilayer films may not be far away from thermodynamic equilibrium. At lower concentrations, film formation is dominated by nonequilibrium effects, and in most cases, Marangoni structures[20] can be identified clearly, as can be seen by optical microscopy in Figure 3a. The so-called Marangoni effect is induced by a concentration gradient that results in an interfacial tension gradient, which initiates a flow of mass along the surface.[21]

The nonequilibrium structures can also be detected by AFM at a lower scan size. Figure 3b,c shows TMAFM pictures of two films influenced by thermodynamical non-equilibrium effects. Figure 3b shows a stripe Marangoni multilayer structure, whereas Figure 3c is more similar to the regular films containing holes, that are found for lower concentrations. These hole structures can be explained firstly by the fact that the concentration does not allow the formation of a complete covering layer. Secondly, due to the crystallization during the slow evaporation process of the solvent, the density of the layer is increased, and consequently there is less surface coverage. In these cases, the molecules are confined to the surface and show domain formation similar to LB films at the air−water interface.[18,19]

The concentrations at which the different topologies (Marangoni stripe structures, monolayer film with hole patterns) of the surface occur depend on the generation of the dendrimer, namely on the weight and the size of the dendrimers, and the type of solvent (i.e. vapor pressure of the solvent). For example, in toluene all processes described take place at approximately 4 times lower concentrations for G1 than for G3 dendrimers. This can be explained by the fact that we measured concentrations in weight percent and the size of the dendrimers is not proportional to their molecular weight, which develops by a power law.

As stated above, this concentration dependence occurs only for solvents with a low vapor pressure (5.3×10^{-4} Pa at 18.4 °C for toluene). For solvents with a high vapor pressure, such as *n*-pentane (2.7×10^{-3} Pa at 18.5 °C), the dendrimers formed flat films without characteristic structures for all the measured concentrations (0.1−0.0007 wt %). The roughness of all the films prepared from an *n*-pentane solution never exceeded 1.5 nm for a $5\,\mu m \times 5\,\mu m$ area. When cast from *n*-pentane, the dendrimers appear to be quenched in a little organized state.

It was not possible, even with TMAFM, to image single dendrimers or clusters of two or three dendrimers without damaging their structure. The force that is applied to the surface deforms the dendrimers, therefore the height of the dendrimer clusters decreases after each scan. The deformability is a well-known problem of the AFM measurement of soft samples and can reduce lateral resolution to several nanometers.[12] However, as described before, at low concentrations, the cellular domain patterns of dendrimer monolayers were found for all generations, when a suitable solvent was used. In the ultrathin films, the dendrimers were clearly more resistant against deformation due to the cohesive interaction within the film.

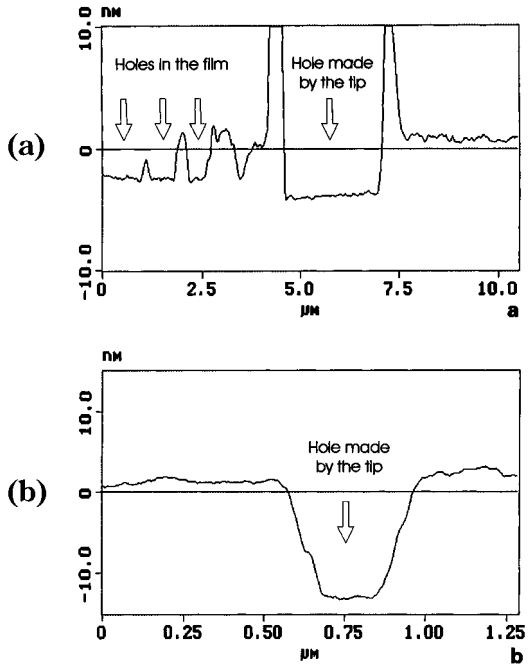

Figure 5. Profiles of TMAFM images of G1 dendrimers cast from toluene: (a) 0.003 wt % and (b) 0.1 wt %.

Table 2. Size of the Three Generations of Dendrimers: Calculated, Measured with AFM, and Measured by WAXD

dendrimer generation	calculated diameter of the dendrimer (nm)	surface layer thickness measured by AFM (nm)	bulk layer spacing measured by WAXS (nm)
G1	4.3	4.4 ± 0.5	4.323 ± 0.002
G2	5.3	4.6 ± 0.5	4.359 ± 0.002
G3	6.6	5.3 ± 0.5	4.413 ± 0.002

Figure 4 shows monolayers of dendrimers of the three generations together with the corresponding height profiles and the distribution of the height of the measured points. From Figure 4 and Table 2 it is obvious that the height of the dendrimer films is well-defined and lies between 4.3 and 5.3 nm with increasing size for higher generations. Similar results were obtained from both TMAFM and CMAFM. Table 2 shows also the calculated maximum sizes of the dendrimer molecules, assuming perfectly extended all-trans chains. The size measured for G1 dendrimers from the monolayers corresponds well to the theoretical value, but both G2 and especially G3 dendrimers lie below the calculated size. However, it has been shown before by WAXS (wide-angle X-ray scattering) measurements on powders of G1−G3 that different generations of the dendrimers form different crystalline structures in the solid state.[10] Despite different packing, in every case, a periodic layer structure of 4.4 nm is found. The AFM measurements therefore correspond reasonably well to the size of the dendrimer layers in the bulk crystal. Thus, we conclude tentatively that similar layer structures are formed

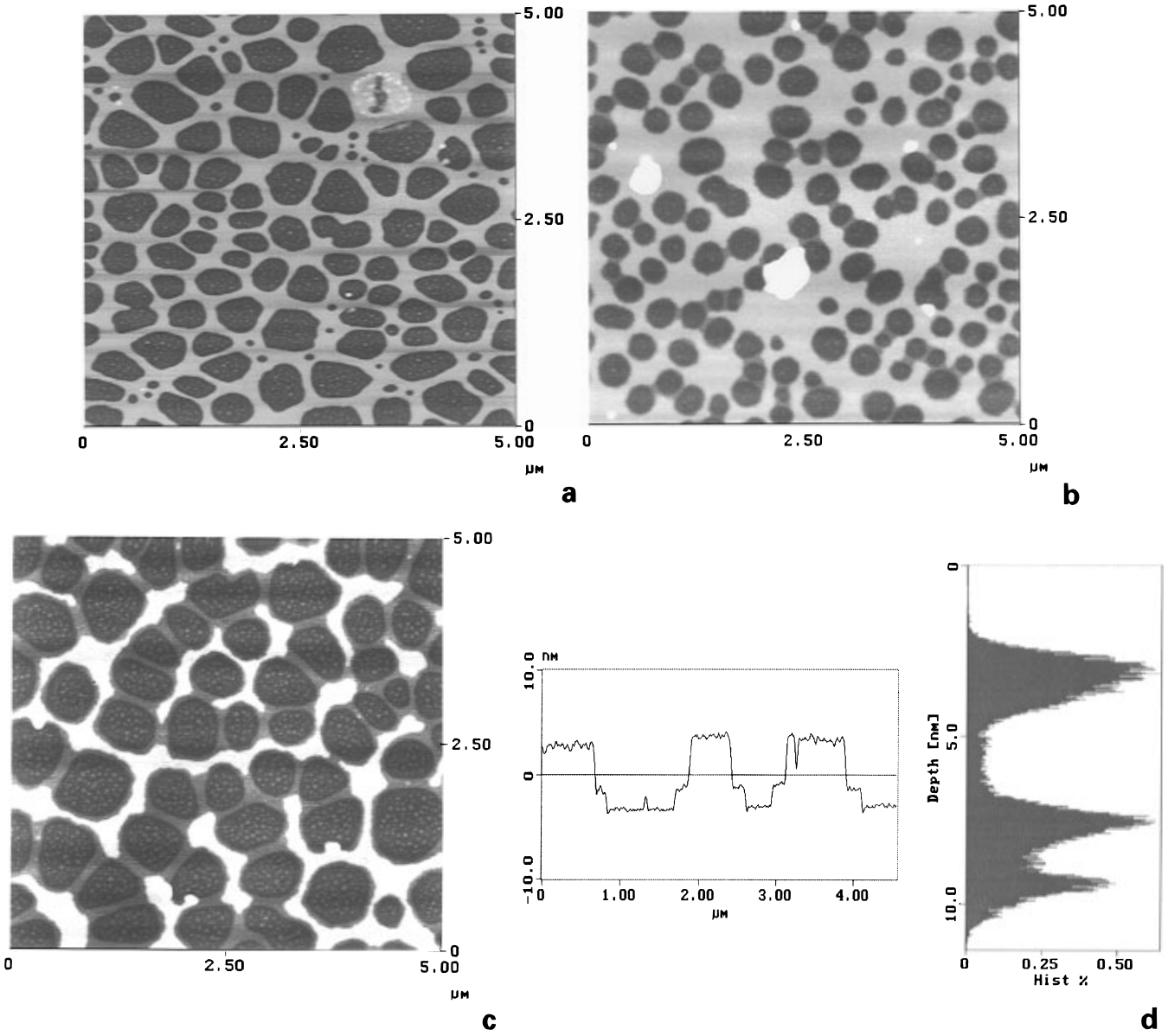

Figure 6. TMAFM images of 0.01 wt % G2 dendrimers in petroleum ether: (a) without annealing, (b) annealed for 10 min at 105 °C, (c) annealed for 4 h and 30 min at 105 °C, (d) profile of the film shown under c.

during the arrangement of dendrimers on a surface and in the bulk phase.

A wealth of domain shapes is observed for the monolayer films of the dendrimers (Figure 4). Circular domains as an equilibrium shape, such as shown in Figure 4a are easily understood if there are no pronounced anisotropic crystal forces and if the boundary is to be minimized for a given domain area. In analogy to LB films of lipids at the air−water interface, the domains appear to grow by a diffusion-limited aggregation process that may lead to fractal structures, as shown in Figures 4b,c.

To confirm the monolayer structure of the deposited films, the dendrimer layer was removed from a small area of the surface by the tip of the CMAFM by scanning with the highest possible force, namely with a setpoint of 10 V. If we consider that the force corresponding to a setpoint of −1.5 V already removes the film, it is legitimate to assume that the highest force will scratch the ultrathin films down to the mica surface. Using this method, we find that the film with holes shown in Figure 5a is composed of a monolayer of dendrimers, since the holes penetrate to the mica surface.

Figure 5b shows that the thickest film, produced with a 0.1 wt % solution, is about 15 nm thick, which corresponds to three monolayers. Therefore, all the measured samples can be regarded as two-dimensional structures.

To study relaxation effects that occur after film formation, the samples were annealed for various periods at 105 °C. Figure 6 shows TMAFM pictures of a G2 monolayer on mica that was (a) non-annealed and (b) annealed for 10 min and (c) several hours. The non-annealed sample forms a continuous film of dendrimers with holes. Figure 6b shows that the holes coalesce in groups of two to five after 10 min of annealing. However, the links between the holes do not represent a complete dewetting of the dendrimer film. Contrary to normal polymer dewetting behavior, a layer of 1−2 nm remains between the holes. After some hours of annealing (Figure 6c), the coalesced holes seem to form a continuous structure, but even after this long annealing time, the thin layer between and around the holes remains unchanged. Further annealing at 150 °C for several hours does not change the surface topology. The profiles of Figure 6d show that the characteristic thick-

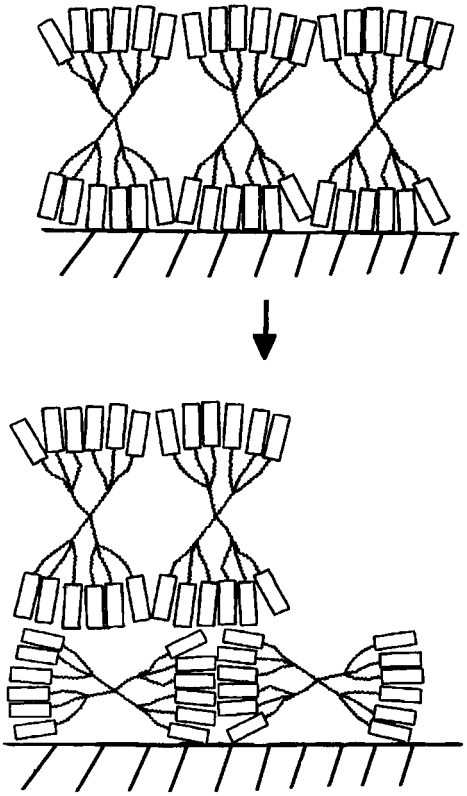

Figure 7. Schematic representation of surface reorientation of G1 and G2 during thermal annealing.

ness of the monolayer is now found between the top surface (highest layer) and the thin layer, and no more between the top surface and the holes, as in Figure 6a. We tentatively explain this by a reorientation process of the dendrimers at the mica surface. The dendrimers become ordered in a first layer, where they are oriented along the surface (1−2-nm), and above it a second layer with an orientation perpendicular to the mica surface (4.5 nm) is formed (Figure 7). Favorable interaction of the carbonate bonds between the mesogens and the carbosilane scaffold with the polar mica surface may be the driving force of a reorientation process of this kind.

Both G1 and G2 dendrimers show similar dewetting behavior. However, G3 was remarkably different and formed extremely flat films that were stable during all annealing experiments. No dewetting or reorientation was observed. We attribute this to the spatial saturation of the dendrimer periphery and resulting low mobility in the third generation. Consequently, the G3 dendrimers show lower mobility and cannot undergo reorientation.

In contrast to the monolayers, multilayer films of G1, G2, and G3 were always stable and did not deform with annealing. Clearly in this case, the cohesion of the layers is too strong to allow a reorientation of the dendrimers at the mica surface.

Conclusion

Mesogen-substituted dendrimers appear to be interesting building blocks for molecularly flat ultrathin organic films. AFM revealed the formation of monolayers as well as flat multilayers, which may be due to the lack of topological constraints, such as entanglements as well as interaction of the mesogenic units in these molecules. For all dendrimer generations, there was a concentration where the films showed rough and completely inhomogeneous surfaces. These surface topographies observed by optical microscopy were found to be similar to structures induced by Marangoni instabilities of the film during solvent evaporation. For low dendrimer concentrations, monolayers were observed. The monolayers showed cellular hole patterns, similar to LB monolayers of lipids at the air−water interface. This may be a general phenomenon for films formed by dendritic macromolecules. The hole structures determined the height of the monolayers of the different dendrimer generations, which correlated well with the size of the bulk crystal layer measured by WAXS. Annealing of G1 and G2 dendrimer films induced reorientation of the dendrimers on the surface.

All three dendrimer generations showed similar film formation behavior in the experiments, except for annealing. The G3 dendrimer, the periphery of which is densely stacked by the cholesteryl groups, did not reorient during annealing of the film. Further studies on carbosilane dendrimers substituted with other mesogens as well as deposition on a variety of substrates are in progress.

Acknowledgment. The financial support of the Fonds der Chemischen Industrie is acknowledged for a scholarship for K.L. as well as financial support for H.F. The Schweizer Nationalfonds made the work possible by granting a scholarship to M.C. Furthermore, we are grateful to the DFG (Deutsche Forschungsgemeinschaft) for financial support.

References and Notes

(1) Halperin, A.; Tirrell, M.; Lodge, T. P. *Adv. Polym. Sci.* **1992**, *100*, 31 and references cited therein.
(2) Patel, S.; Tirrell, M. *Annu. Rev. Phys. Chem.* **1989**, *40*, 597 and references cited therein.
(3) Hashimoto, T. Structure of Polymer Blends. In *Materials Science and Technology*; Thomas, E. L., Ed.; VCH: Weinheim, 1993; Vol. 12.
(4) Fleer, G. J.; Cohen-Stuart M. A.; Scheutjens, H. M.; Cosgrove, T.; Vincent, B. In *Polymers at Interfaces*; Chapman & Hall: London, 1993.
(5) Tomalia, D. A.; Durst, H. D. *Top. Curr. Chem.* **1993**, *165*, 193.
(6) Newkome, G. R.; Moorefield, C. N.; Baker, G. R.; Johnson, A. L.; Behera, R. K. *Angew. Chem.* **1991**, *103*, 1205−1209.
(7) Watanabe, S.; Regen, S. L. *J. Am. Chem. Soc.* **1994**, *116*, 8855.
(8) Kowalewski, T.; Wooley, K.; Hawker, C.; Fréchet, J. Abstracts Macro-Akron Symposium, 1994, p 327.
(9) Sheiko, S. S.; Eckert, G.; Ignat'eva, G.; Muzafarov, A. M.; Räder H. J.; Möller, M. *Macromol. Rapid Commun.* **1996**, *17*, 283.
(10) Frey, H.; Lorenz, K.; Mülhaupt, R. Rapp, U.; Mayer-Posner, F. J. *PMSE Proc. ACS-Meeting Chicago* **1995**, *73*, 127. Lorenz, K.; Hölter, D.; Stühn, B.; Mülhaupt, R.; Frey, H. *Adv. Mat.* **1996**, *8*, 414. Lorenz, K.; Hölter, D.; Frey, H.; Mülhaupt, R., submitted.
(11) Wawkuschewski, A., Crämer, K., Cantow H.-J., Magonov, S. N. *Ultramicroscopy* **1995**, in press.
(12) Radmacher, M.; Tillmann, R. W.; Fritz, M.; Gaub, H. E. *Science* **1992**, *257*, 1900.
(13) van der Made, A. W.; van Leeuwen, P. W. N. M. *J. Chem Soc. Chem. Commun.* **1992**, 1400.
(14) Zhou, L. L.; Roovers, J. *Macromolecules* **1993**, *26*, 963−968.
(15) Lorenz, K.; Mülhaupt, R.; Frey, H.; Rapp, U.; Mayer-Posner, F. J. *Macromolecules* **1995**, *28*, 6657.
(16) Wang, Ch.; Kressler, J.; Kammer, H. W. *Langmuir*, submitted.
(17) Smithson, R. L. W.; Stange, T. G.; Evans, D. F.; Edstrom, R. D.; Henddrick-son, W. A. *AIP Conf. Proc.* **1992**, *241 (Scanning Probe Microsc.)*, 219.
(18) Seul, M.; Andelman, D. *Science* **1995**, *267*, 476.
(19) Möhwald, H. *Annu. Rev. Phys. Chem.* **1990**, *41*, 441.
(20) Köhler, J. M.; Weh, L. *Makromol. Chem.* **1991**, *192*, 1147. Weh, L. poster presentation at the Potsdam workshop on thin organic films, May 1995.
(21) Dukhin, S. S.; Kretzschmar, G.; Miller, R. *Dynamics of Adsorption at Liquid Interfaces*, Möbius, D., Miller, R., Eds.; Elsevier: Amsterdam, 1995.

MA951545U